SOME ASPECTS OF THE HETEROGENEOUS PRECIPITATION OF THE METASTABLE γ'' PHASE IN ALLOY 625

M. Sundararaman, R. Kishore and P. Mukhopadhyay

Metallurgy Division
Bhabha Atomic Research Centre
Bombay 400 085, India

Abstract

The commercial nickel base superalloy Alloy 625 can be strengthened by the precipitation of the metastable γ'' phase (DO_{22} structure) which is based on the stoichiometry Ni_3Nb. Suitable ageing treatments in the temperature range of 600°C to 800°C can bring about copious γ'' precipitation in this alloy, the mode of precipitate nucleation depending on the aging temperature. At relatively low temperatures γ'' particles nucleate homogeneously in the austenite matrix. Ageing at temperatures above 800°C (and prolonged aging at somewhat lower temperatures) brings about the precipitation of the equilibrium intermetallic δ phase (DO_a structure; Ni_3Nb stoichiometry). When ageing is carried out at temperatures close to but lower than the γ'' solvus temperature, the γ'' phase precipitates in a predominantly heterogeneous manner, dislocations and coherent twin boundaries being the preferred nucleation sites. The nucleation of all the three variants on dislocations has been observed. An attempt has been made to rationalise this observation by taking into consideration factors such as the elastic interaction between the strain fields of the dislocations and the γ'' precipitates and the stacking fault energy of the austenite matrix. The transition in the γ'' precipitation mode – from homogeneous to heterogeneous – with increasing aging temperature has been discussed in terms of the available time–temperature–precipitation (TTP) curves corresponding to the formation of intermetallic phases in this alloy.

Superalloys 718, 625, 706 and Various Derivatives
Edited by E.A. Loria
The Minerals, Metals & Materials Society, 1994

Introduction

The commercial nickel base superalloy Alloy 625 has high strength and toughness from cryogenic temperatures upto 1100°C and is endowed with exceptional fatigue strength and good resistance to chloride ion stress corrosion cracking [1]. At high temperatures, this alloy derives its strength mainly from solid solution hardening [2] while at intermediate temperatures strengthening is brought about mainly by the precipitation of the metastable γ" phase (Ni_3Nb) which has the body centred tetragonal DO_{22} structure [3,4]. The γ" phase forms on ageing at temperatures above 600°C. The equilibrium intermetallic phase in this alloy is the orthorhombic δ – Ni_3Nb phase (DO_a structure). The formation of the δ phase either directly from the supersaturated solid solution at high temperatures or by the replacement of metastable γ" particles on prolonged ageing at lower temperatures has been reported earlier [5].

When a supersaturated solid solution is aged, second phase particles nucleate homogeneously within the matrix or heterogeneously on imperfections such as grain boundaries, twin boundaries and dislocations, depending upon the temperature of ageing and the degree of supersaturation of the parent phase [6]. Equilibrium phases often nucleate at grain boundaries [7,8] while dislocations also act as effective nucleation sites for heterogeneous precipitation [6,9]. When the degree of supersaturation is low and an appreciable reduction in the volume strain energy is associated with nucleation, metastable phases may nucleate preferably on dislocations [10]. Heterogeneous nucleation can occur at the core as in the case of incoherent precipitation [11,12] and also in the strain field of the dislocation as in the case of coherent nucleation [13,14]. This paper reports the results of a detailed investigation on the mode of nucleation of γ" particles as a function of ageing temperature and time. The present results on the transition in the mode of γ" phase precipitation from homogeneous to heterogeneous, as a function of the ageing temperature, has been discussed in terms of the available TTP curves corresponding to the formation of intermetallic phases in this alloy.

Experimental Procedure

The chemical composition of the Alloy 625 used in this work is shown in Table I. Samples, encapsulated in silica tubes under helium atmosphere, were solution treated at 1100°C for 1 h and then water quenched. Subsequently these samples were aged at temperatures in the range of 600°C to 900°C for various periods of time to precipitate intermetallic phase precipitates. Sample preparation for TEM has been described elsewhere[14].

Table I. Chemical Composition of Alloy 625

Element	Ni	Cr	Mo	Nb	Fe	Al	Ti	Co	Mn	Si	C
Conc.wt%	61.9	21.0	9.05	3.7	3.5	0.17	0.23	0.08	0.14	0.15	0.05
Conc.at%	62.6	24.2	5.6	2.4	3.8	0.38	0.29	0.08	0.15	0.34	0.25

Conc. – concentration; wt% – weight percent; at% – atomic percent

Figure 1 – Solution treated microstructure revealing planar array of dislocations along {111} planes.

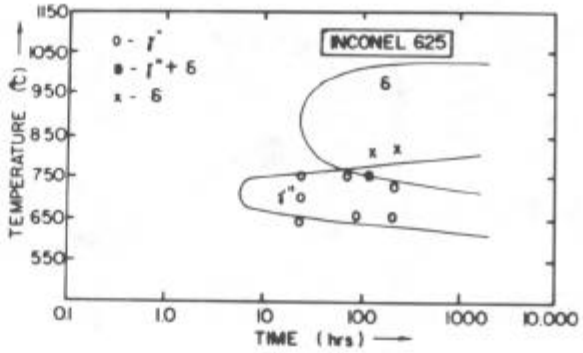

Figure 2 – Time– temperature precipitation (TTP) diagram corresponding to γ" and δ precipitation in Alloy 625[19]. Data corresponding to present work are marked in the figure.

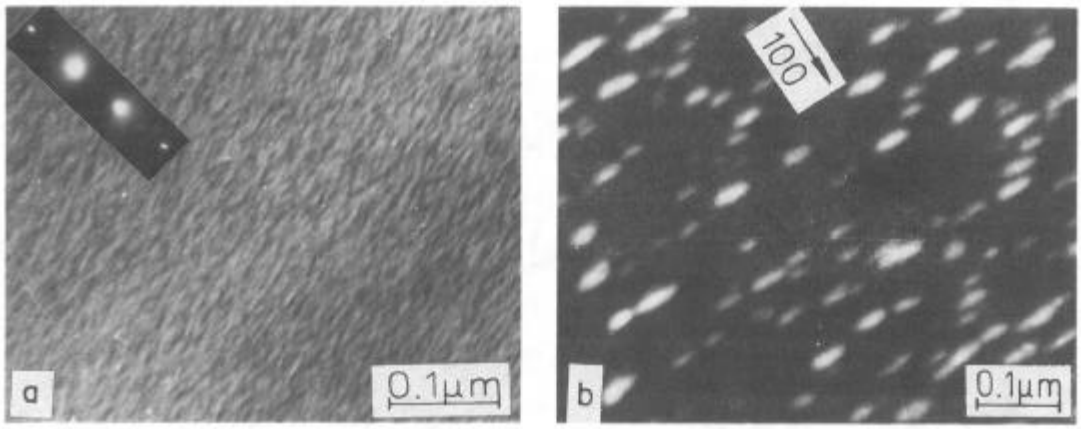

Figure 3 – (a) Mottled contrast in bright field micrograph indicating homogeneous precipitation of γ" in samples aged at 650°C for 6 h.(b) Dark field image with an {100} reflection showing the presence of only ellipsoidal γ" particles.

Results

Solution treated and quenched samples revealed quite a high density of dislocations which were arranged in planar arrays (Fig. 1). These dislocations could have been generated due to the high quenching stresses present in the material. Stereographic analysis revealed that the planar arrays were confined to the {111} planes.

Ageing of solution treated samples in the temperature range of 600°C to 900°C resulted in the formation of intermetallic phases. As in the case of Inconel 718 [15], the precipitating phases in this alloy were identified from their morphologies as well as from the presence of distinct superlattice spots corresponding to them in selected area diffraction patterns. At low temperatures ellipsoidal precipitates of the metastable γ" phases formed while at high

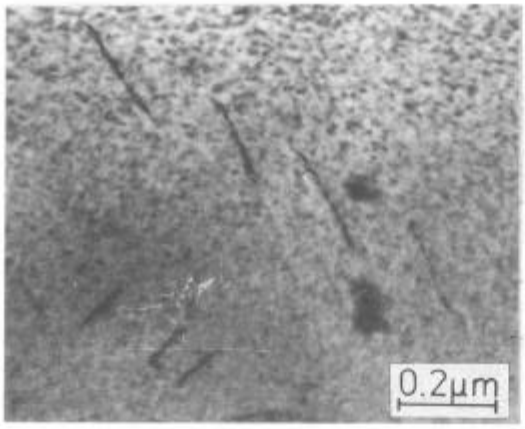

Figure 4 – Heterogeneous nucleation of γ" particles (marked by arrows) on dislocations in Alloy 625 aged at 700°C for 24 h.

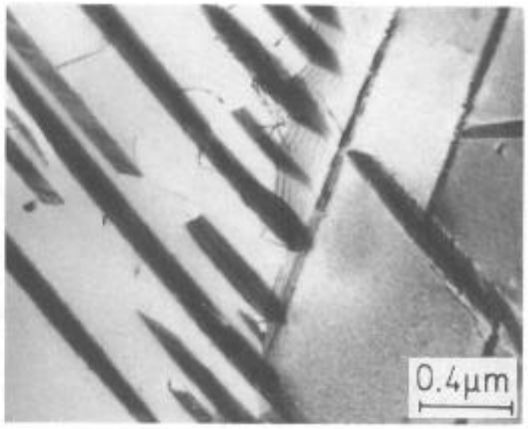

Figure 5 – Occurrence of needle shaped δ phase precipitates within the matrix as well as at grain boundaries in Alloy 625 aged at 750°C for 240 h.

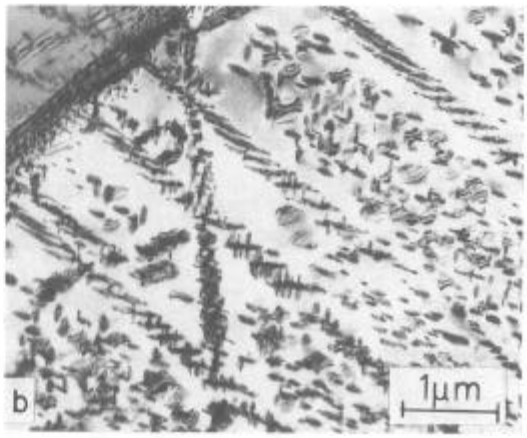

Figure 6 – (a) Heterogeneous precipitation of γ" particles along dislocation lines in solution treated samples deformed to 2% plastic strain in tension and then aged at 750°C for 24 h. (b) Homogeneous and heterogeneous nucleation of γ" particles in a sample aged at 725°C for 200 h.

temperatures, needle shaped precipitates of the equilibrium δ phase formed. The sequence of precipitation in this alloy was quite similar to that observed in Inconel 718 [16,17]. As indicated in Fig. 2, the observations made in this work were in conformity with the TTP plots for Alloy 625 reported by earlier workers [18,19]. It could be seen from the figure that the γ" phase precipitates over a rather narrow temperature range of 600°C to 800°C in this alloy and that the region of overlap between the TTP curves corresponding to the γ" and the δ phases is restricted to a small region very close to the γ" solvus. Some details of γ" precipitation in this alloy are reported in the following sub–sections. For the ageing temperatures employed in this work, carbide precipitation was found to occur profusely at grain boundaries and incoherent segments of twin boundaries and this aspect will be reported elsewhere.

Microstructure of aged alloy

Precipitation at temperatures upto 700°C. The response of Alloy 625, in respect of γ" precipitation, to ageing at temperatures upto 700°C was found to be qualitatively similar to that of Inconel 718 [15]. Very fine ellipsoidal γ" particles were homogeneously distributed in the matrix in samples aged at lower temperatures (eg., 650°C). The number density of the precipitates was very high and the large coherency strain associated with these γ" particles produced a mottled contrast in bright field images obtained under dynamical imaging conditions (Fig. 3(a)). In samples subjected to prolonged ageing at these temperatures, the γ" precipitates could be clearly resolved in bright field and they could also be imaged in dark field with superlattice reflections corresponding to the γ" phase (Fig. 3 (b)). No precipitates with a spherical morphology could be seen in dark field images obtained with {100} reflections for any of the ageing treatments employed in this study, indicating the absence of γ' precipitation in this alloy.

Ageing at 700°C, accelerated the growth kinetics of γ" precipitates. Matrix dislocations were quite often found to be decorated with γ" particles (Fig. 4). At these ageing temperatures δ phase precipitation did not occur in this alloy even on prolonged ageing. However, it readily occurred on ageing at temperatures above 750°C (Fig. 5). The details of δ precipitation in Alloy 625 have been reported earlier [5].

γ" precipitation at temperatures above 700°C. On ageing at temperatures above 700°C, preferred nucleation of γ" particles at structural singularities like dislocations and twin boundaries became very pronounced. Some typical features of the corresponding microstructure are illustrated in Fig. 6. A comparison of this microstructure with that of the solution treated alloy revealed that precipitation had occurred on dislocations which were arranged in planar arrays along the {111} planes. Individual precipitates could not be resolved very clearly. In some regions, the γ" precipitation on dislocation had the appearance of leaves on stems (Fig. 7). Precipitation on dislocations was generally quite uniform and a great

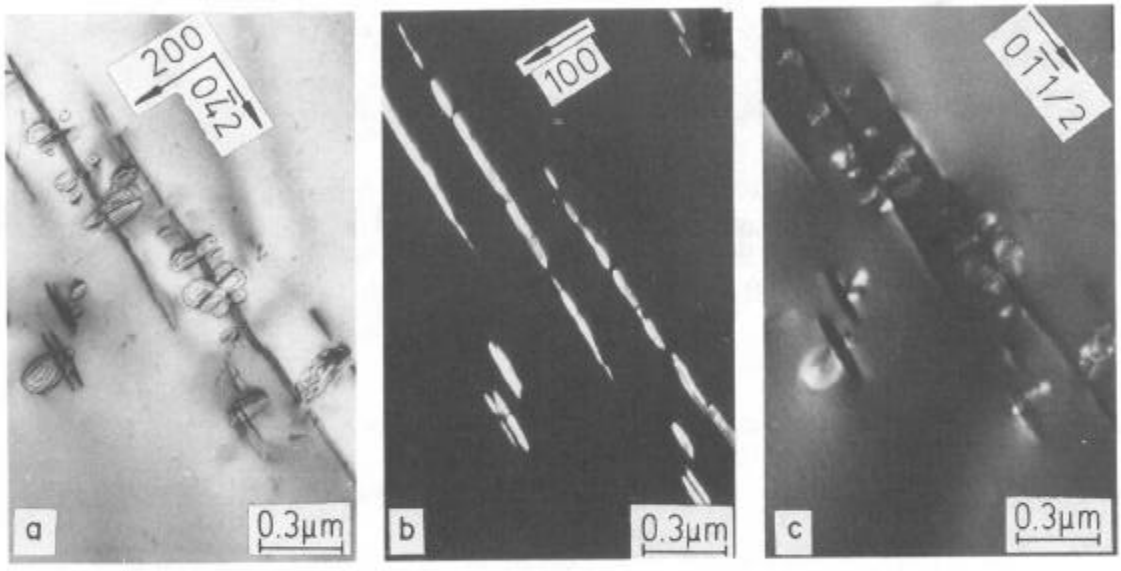

Figure 7 – The appearance of leaves on stem morphology of γ" precipitates nucleated on dislocations in Alloy 625 aged at 750°C for 100 h. (a) Bright field micrograph; (b) and (c) are dark field micrographs with (100) and (0 $\bar{1}$ 1/2) superlattice reflections respectively. [012] zone axis.

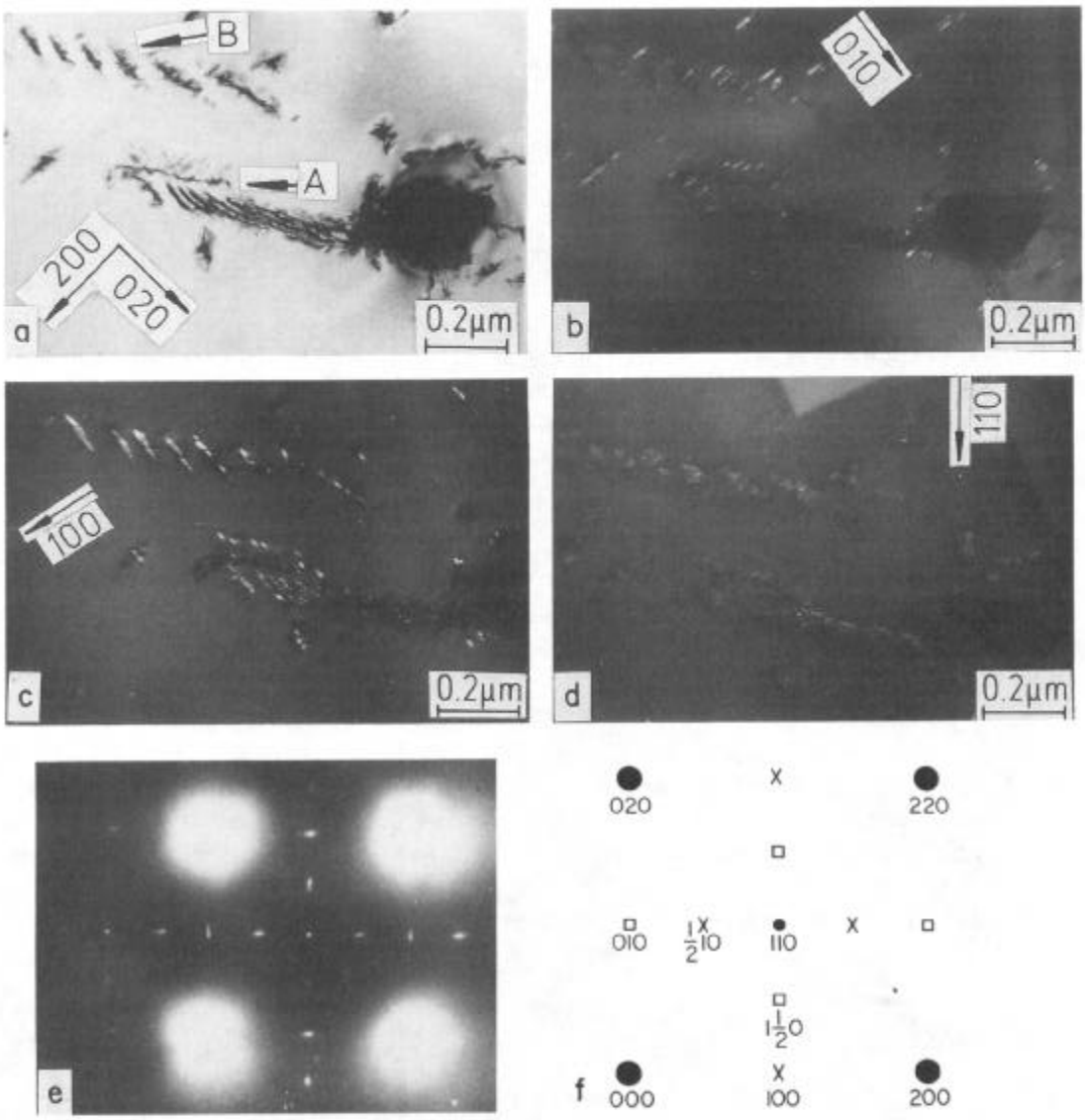

Figure 8 – Heterogeneous precipitation of γ" precipitates belonging to all the three variants on dislocations in Alloy 625 aged at 750° C for 24 h.(a) Bright field micrograph; (b), (c) and (d) are dark field images of [010], [100] and [001] variants respectively, imaged using (010), (100) and (110) reflections; (e) corresponding [001] zone axis SAD pattern; (f) key to SAD pattern in (e). The micrographs correspond to the same area of the sample.

majority of the dislocations were decorated with a large number of precipitates. Regions of the austenite matrix surrounding such heterogeneously nucleated γ" precipitate clusters appeared to be free from homogeneously nucleated γ" particles.

The different γ" precipitate variants nucleating on dislocations were identified by imaging them in dark field using superlattice reflections. It was found that all the three variants could nucleate in the vicinity of dislocations (Fig. 8). This was indicated by the presence of superlattice reflections corresponding to all the three γ" variants in [001] zone axis SAD patterns obtained from regions containing such heterogeneously nucleated γ" precipitates. In

Fig. 8 (a), in the region marked A, the projected dislocation line vector is along the $[1\bar{1}0]$ direction while in the region B, the projected dislocation line vector is along the [010] direction. It could also be seen that in the region A, the [100] and the [010] variants (i.e., γ'' variants with the c–axis along [100] and [010] directions respectively of the austenite matrix) are inclined with respect to dislocation lines whereas in region B, the [001] variant is parallel with respect to dislocation lines. In order to ascertain whether precipitation in these regions was on edge or on screw dislocations, a set of schematic diagrams were constructed to indicate the angular relations between Burgers vectors and dislocation line vectors for all possible 1/2<110> type dislocations and directions normal to the habit plane of the different precipitate variants. A direct comparison between these schematic drawings (Fig. 9) and the observed geometry of precipitation in the vicinity of dislocations (Fig.8) could be made by assuming the dislocations to the either of pure screw or of pure edge type. This assumption was valid in this instance because the observed projections of the dislocation lines were straight and were either parallel or perpendicular to one or other of the <110> vectors. It could be inferred from this comparison that the precipitate geometry in region A corresponded to precipitation on either edge or screw dislocations while that in region B corresponded to precipitation on only screw dislocations. The heterogeneous mode of precipitation in this case did not alter the γ'' precipitate habit plane. Even though all the γ'' precipitate variants could nucleate on a dislocation, the number density of particles belonging to any given variant appeared to vary from dislocation to dislocation suggesting that the potency of a dislocation for nucleation of different variants on it may be different. Quantitative estimation of the nucleation density corresponding to each of the γ'' variants was not attempted.

In addition to precipitation on dislocations, γ'' particles were observed to be heterogeneously nucleated on coherent twin boundaries (marked by arrows in Fig. 10 (a)). The γ'' precipitates on the matrix side as well as those on the twin side could be brought into contrast separately or simultaneously and appeared to be abruptly terminated at the twin interface (Fig.10(b), (d)). These twin boundary nucleated γ'' precipitates grew with increasing ageing time (Fig.10(c)). It appeared that the particles nucleated in the same region of the boundary and subsequently grew into the matrix as well as into the twin.

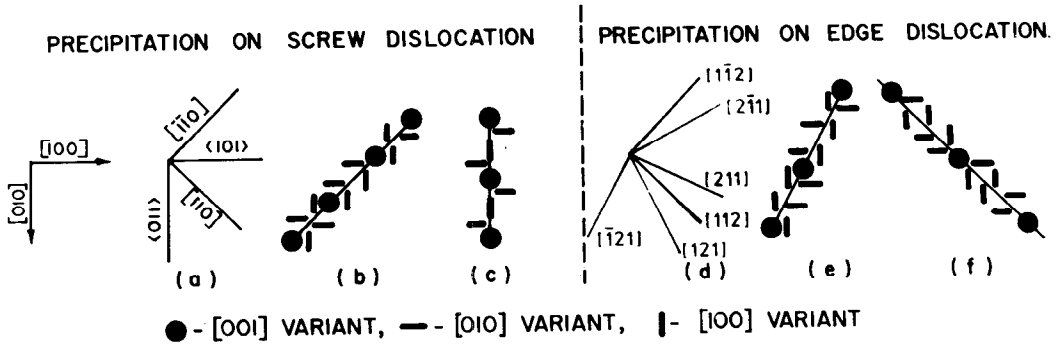

Figure 9 – Schematic diagram showing nucleation of γ'' particles on dislocations. Line directions for screw and edge dislocations with Burgers vectors 1/2<110> as projected on the (001) plane are shown in (a) and (d) respectively; (b), (c), (e) and (f) indicate nucleation of γ'' variants on projected dislocation line directions.

Discussion

The sequence of precipitation of intermetallic phases in this alloy, except for the total absence of γ' precipitation, was very similar to that observed in Inconel 718 [17]. The observed intermetallic phase precipitation sequence and the reported TTP diagrams (Fig.2) pertaining to Alloy 625 have been rationalised in terms of the relative magnitudes of the nucleation barriers with regard to the γ'' and the δ phases as in the case of Inconel 718 [16,17]. The absence of γ' precipitates in Alloy 625 would be explained qualitatively in terms of the free electron model proposed by Sinha [20]. Alloy 625 is lean in iron, aluminium and titanium and richer in molybdenum as compared to Alloy 718. As a result, the reduction in the electron concentration appears to be insufficient to induce the formation of the γ' phase, though it is adequate to bring about γ'' precipitation [17]. It should be pointed out in this context that Garzarotli et al.[4] did not observe precipitation in an Alloy 625 alloy in which aluminium and titanium were absent. This suggests that the small amounts of titanium and aluminium present in Alloy 625 are necessary for the formation of the γ'' phase.

Homogeneous versus heterogeneous nucleation

Microstructural observations clearly indicated that the nucleation of γ'' precipitates was homogeneous upto an ageing temperature of 650°C whereas heterogeneous nucleation on and in the vicinity of dislocations was very pronounced at 750°C. This change in the mode of precipitation has been qualitatively explained earlier in terms of the ratio of the rates of heterogeneous and homogeneous nucleation [14] which is given by the following relation [6]:

$$\frac{J_{het}}{J_{hom}} = \frac{N_{het}}{N_{hom}} \exp - \frac{(\Delta G_{het} - \Delta G_{hom})}{kT} \qquad \text{——(1)}$$

where J is the nucleation rate, N is the number density of potential nucleation sites, ΔG is the activation energy for the formation of a critical nucleus and the subscripts 'het' and 'hom' refer respectively to heterogeneous and homogeneous nucleation processes. Under certain conditions homogeneous nucleation can dominate over heterogeneous nucleation in spite of the fact that ΔG_{het} is always smaller than ΔG_{hom} [6]. This is because $N_{hom} >> N_{het}$. For homogeneous nucleation to become competitive with heterogeneous nucleation the value of the exponential term should be much less than that of the ratio N_{hom}/N_{het}. Such a situation can arise only if the free energy barrier for nucleation is very small. In view of the observations made in the present work, one could conclude that this condition was satisfied at temperatures lower than 650°C, where the high solute supersaturation of the matrix led to the required depression of the activation barrier for nucleation. As pointed out earlier and as shown in Fig.2, the region of overlap between the TTP curves corresponding to the precipitation of the γ'' and the δ phases is narrow and is restricted quite near the solvus line of the γ'' phase. This was the reason why it was possible in this alloy to get an access to a temperature range where the supersaturation with respect to the γ'' phase was low and at the same time the competing process of δ phase precipitation could not operate. In this temperature range, heterogeneous nucleation of the γ'' phase was favoured.

Nucleation on dislocations

Preferential nucleation of precipitates at dislocations occurs when the driving force for nucleation (which depends on the extent of supersaturation) is not very large [13].

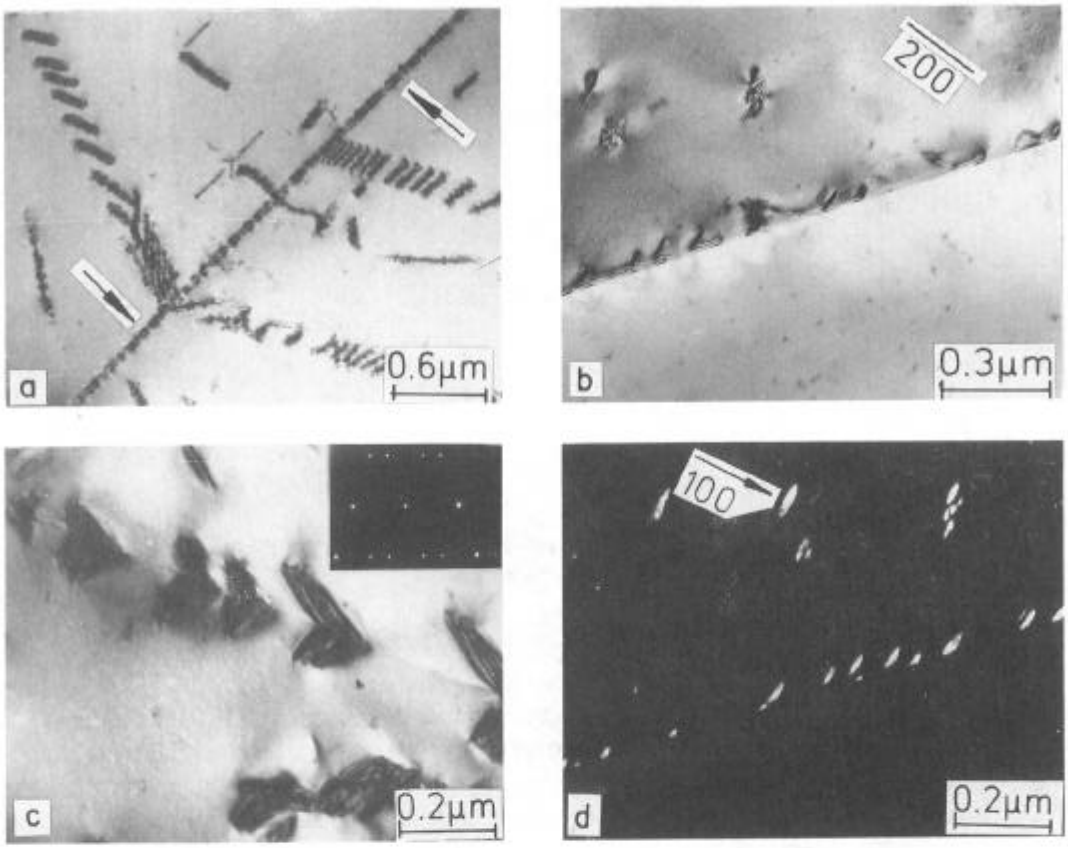

Figure 10 – (a) Heterogeneous precipitation of γ" particles on coherent twin boundaries (marked by arrows) and dislocations;(b) and (d) are bright field and dark field (with (001) superlattice reflection) micrographs respectively showing the nucleation of γ" precipitates on only one side of a twin boundary; (c) γ" precipitates nucleated at and growing into either side of a twin boundary. Inset in (c) shows the corresponding <110> zone axis diffraction pattern corresponding to fcc twins.

Considerations based on the magnitude of the elastic interaction between the strain fields associated with dislocations and with precipitates and on the experimental observations[21,22] indicate that in the context of precipitate nucleation on dislocations, edge dislocations are more effective nucleation sites than screw dislocations and that all habits of a precipitate phase are not nucleated on one dislocation; the variants that do nucleate are those for which the reduction in strain energy is a maximum. In the case of γ" precipitation on an 1/2[1$\bar{1}$0] dislocation in the matrix, out of the three γ" variants, the one with the tetragonal axis parallel to the [001] direction would have no elastic interaction with the dislocation. The nucleation of γ" precipitates belonging to this variant on this dislocation would be unlikely. However, the observations made in the present work demonstrated that the precipitates belonging to all the three variants appeared at the vicinity of edge as well as screw type dislocations with 1/2<110> Burgers vectors. In order to rationalise this observation, a detailed analysis of dislocation precipitate elastic interaction was carried out.

Some simplifying assumptions were made in the analysis. These were: (i) the shear moduli of the matrix and the precipitate phases are the same; (ii) the matrix is elastically isotropic; (iii) the linear elasticity theory is applicable and (iv) no strong elastic interaction exists

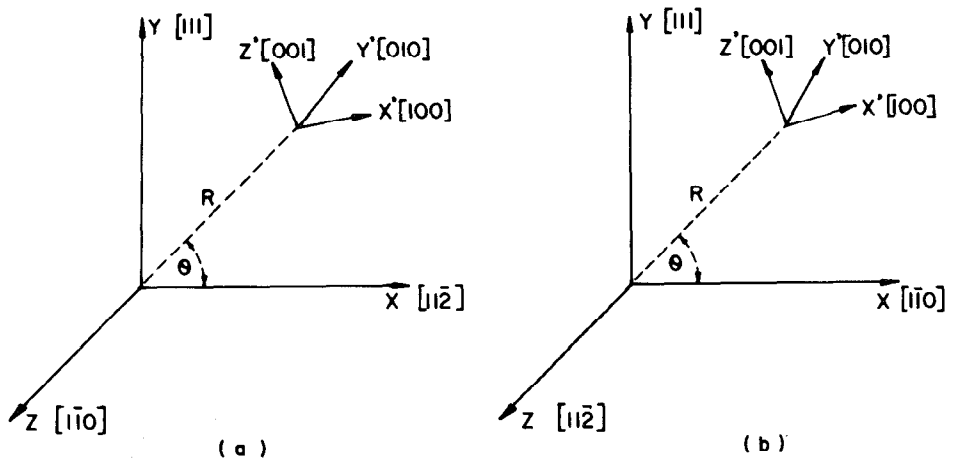

Figure 11 – Co–ordinate system chosen for (a) screw and (b) edge dislocations.

between the strain fields of the neighbouring precipitates. The elastic interaction energy was estimated by assuming that the stress field of the dislocation interacted with the strain field of the precipitate[23,24] and that it did not vary appreciably over the small volume of the precipitate nucleus. The assumption of a non varying stress field was reasonable as long as the precipitate was located outside the dislocation core. With these assumptions, the procedure for the calculation of the elastic strain energy was quite similar to that employed in describing solid solution strengthening arising from misfitting atoms or defects[25–27].

The interaction energy, E, between a dislocation and a misfitting particle is given by the relation:

$$E = - \sigma_{ij} e_{ij} V \qquad \text{——(2)}$$

where σ_{ij} is the dislocation stress field at the centre of the precipitate and e_{ij} is the homogeneous stress free strain associated with the particle of volume V. The co– ordinate systems chosen for screw and edge dislocations are shown in Fig.11. The z–axis is along the dislocation line vector, the y–axis is along the [111] direction and the x–axis is along the vector perpendicular to the plane containing the y– and the z– axes. The transformation from the precipitate co–ordinate system to the dislocation co–ordinate system could be expressed as $e_{ij} = l_{mi} l_{jn} e'_{mn}$, where l_{mi} are the elements of the co–ordinate transformation matrix. The transformation matrices for changing over from the precipitate to the dislocation co–ordinate system for edge and screw dislocations respectively are given by:

$$\begin{bmatrix} 1/\sqrt{2} & 1/\sqrt{3} & 1/\sqrt{6} \\ -1/\sqrt{2} & 1/\sqrt{3} & 1/\sqrt{6} \\ 0 & 1/\sqrt{3} & -2/\sqrt{6} \end{bmatrix} \quad \text{and} \quad \begin{bmatrix} 1/\sqrt{6} & 1/\sqrt{3} & 1/\sqrt{2} \\ 1/\sqrt{6} & 1/\sqrt{3} & -1/\sqrt{2} \\ -2/\sqrt{6} & 1/\sqrt{3} & 0 \end{bmatrix}$$

The interaction energies for all the three γ" variants were evaluated using eqn.(2) by transforming the precipitate strain field with respect to the dislocation co– ordinate system. The small strains in the plane normal to the tetragonal axis were neglected in the present

Table II. Expressions for the elastic energy of interaction between the strain field of a γ" precipitate and the stress field of an a/2 [1$\bar{1}$0] dislocation

Case	Nature of dislocation	Angle between c–axis of γ" and Burgers Vector of dislocation	Elastic interaction energy
1	Screw	45°	$A\left(\frac{\sqrt{2}\,\mathrm{Cos}\theta - \mathrm{Sin}\theta}{\sqrt{3}\,R}\right)$
2	Screw	90°	0
3	Edge	45°	$-A\left(\frac{6\sqrt{6}\mathrm{Cos}^3\theta + 23\mathrm{Cos}^2\theta\mathrm{Sin}\theta - 6\sqrt{6}\mathrm{Cos}\theta\,\mathrm{Sin}^2\theta + 17\mathrm{Sin}^3\theta}{12\,R}\right)$
4	Edge	90°	$-A\left(\frac{7\mathrm{Sin}^3\theta + \mathrm{Cos}^2\theta\mathrm{Sin}\theta}{6\,R}\right)$

$A = \mu b \epsilon V/2$; μ = shear modulus; b = Burgers vector of dislocation;
ϵ = stress free strain along tetragonal axis of precipitate;

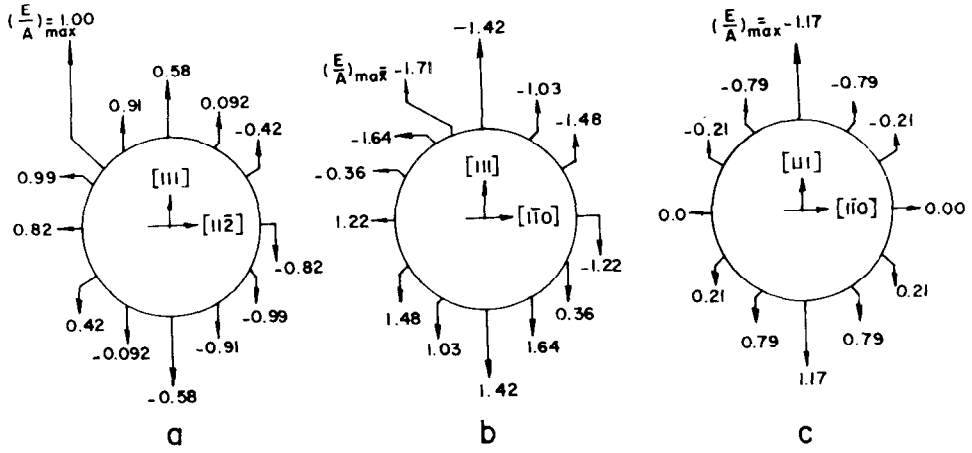

Figure 12 – Estimated values of the elastic interaction energy for the nucleation of γ" particles at different positions around a matrix dislocation. (a) [100] and [010] variants around an 1/2[1$\bar{1}$0] screw dislocation; (b) and (c) between 1/2[1$\bar{1}$0] edge dislocation and [100] and [001] variants respectively.

analysis. The calculations were fairly straightforward, though somewhat cumbersome. The results of the calculations have been presented in terms of cylindrical co– ordinates, by assuming the relationships $x = R\cos\theta$, $y = R\sin\theta$ and $z = z$, in Table II. Four cases have been considered, depending on the nature of the dislocation and the orientation of the precipitate with respect to the dislocation Burgers vector.

The values of E/A (the quantity A defined in table II is a constant in this case and has the same dimensions as that of E) were numerically computed for various values of θ for a constant distance R of the centre of the precipitate from dislocation core and the results are illustrated in Fig. 12. On the basis of these results , the following conclusions could be drawn: (1) The interaction energy increases with increasing values of misfit parameter in all cases. (2) The maximum of interaction energy occurs for particular position of the precipitate around the dislocation core. For e.g., in case 3, the elastic interacting energy has a maximum value when the centres of the precipitates are located along that <132> direction which makes an angle of 68° with dislocation with $b = 1/2[1\bar{1}0]$. (3) The maximum value of E/A for the same value of R corresponding to cases 1, 3, and 4 are respectively in the ratio 1: 1.71: 1.17. This suggests that case 3 (the tetragonal axis of the precipitate makes an angle of 45° with respect to edge dislocation with $b = 1/2[1\bar{1}0]$) provides the maximum advantage for dislocation associated heterogeneous nucleation.

This calculation reveals that all the three variants of γ'' precipitates can form on an edge dislocation while only two γ'' variants can nucleate on screw dislocation. However, Bapna and Parameswaran [28] have shown that an attractive interaction takes place between a defect with tetragonal strain along [001] direction and an $1/2[1\bar{1}0]$ screw dislocation when the dislocation is dissociated. The arrangement of dislocations in planar arrays in this alloy is suggestive of the fact that the stacking fault energy of the matrix has an intermediate value[29]. Hence the dissociation of dislocations into partials separated by very small distances (possibly of the order of the resolution limit of the TEM observations) could not be ruled out. The occurrence of such splitting could be responsible for the precipitation of all three γ'' variants in the vicinity of screw dislocations.

The elastic interaction due to the difference in the elastic moduli of the matrix and the precipitate phases may influence heterogeneous nucleation close to dislocations. If the elastic modulus of the precipitate phase is larger than that of the matrix, the creation of a precipitate in the stress field of a dislocation would cause an increase in its strain energy[30]. In other words, such precipitates would experience repulsive forces from dislocations due to this modulus effect. Due to the opposing effects of strain interaction and modulus difference, the precipitates would nucleate at some distance from the dislocation lines. The precise estimation of these distances would require a knowledge of the elastic moduli of the matrix and the precipitate phases and these values are not available. The value of the elastic modulus of γ'' phase could have been larger than that of the matrix and the present experimental observations appear to be consistent with the qualitative description presented here.

Nucleation on coherent twin boundaries

Copious precipitation of γ'' particles on coherent twin boundaries could be observed in this alloy on ageing at temperatures close to the γ'' solvus temperature. The $\{111\}_\gamma$ planes were the coherent twin boundary planes and they are also the close packed planes of the matrix. The atomic arrangement on these planes was identical to that on the close packed planes of the γ'' precipitates, but for the presence of order in the latter. This similarity between the close packed γ'' planes and the coherent twin boundary planes appeared to make the precipitation

of the γ" phase on coherent twin boundaries possible. Moreover the energy of the coherent twin boundary area consumed by γ" precipitation would be available to reduce the overall free energy barrier associated with γ" nucleation. Because of the good lattice registry between the precipitates and the twin related austenite crystals, the interfacial energy would not increase appreciably. At small supersaturations, the critical nucleus size would thus be smaller for twin boundary nucleation than for homogeneous nucleation. This mode of heterogeneous nucleation would, therefore, be favoured at temperatures close to but lower than the γ" solvus temperature. The γ" particle densities on coherent twin boundaries and on dislocations appeared to be of comparable magnitudes, indicating that in low supersaturation situations, both these types of sites were almost equally favoured for precipitate nucleation. In some regions along coherent twin boundaries pairs of twin related γ" precipitates were found to form. Such a precipitate geometry was possible because the appropriate γ – γ" orientation relationship was satisfied on either side of the interface separating the twin related austenite crystals. Since the boundary between the two adjoining precipitates was a twin boundary, the energy associated with this interface would be comparable to, if not smaller than, that associated with the pre–existing austenite twin boundary consumed during precipitation.

Conclusions

On the basis of the results reported in this paper, the following conclusions could be drawn:

1. At low supersaturations, heterogeneous nucleation of γ" precipitates occurs extensively on dislocations and on coherent twin boundaries.

2. All the three variants of γ" particles precipitate heterogeneously on edge and screw dislocations. This observation has been rationalised on the basis of estimation of the precipitate– dislocation elastic interaction energy.

Acknowledgements

The authors are thankful to Dr. S. Banerjee, Head, Metallurgy Division for many useful discussions. The authors are indebted to Dr. C. K. Gupta, Director, Materials Group for his constant encouragement and support.

References

1. H. E. Chandler and D. F. Baxter, " Trends in Superalloys Technology", Metal Progress, 119 (1981), 44–46.
2. D. R. Muzyka, " The Metallurgy of Nickel Iron Alloys", Superalloys, ed., C. T. Sims and W. C. Hagel (John Wiley and Sons, New York, 1972), 113–143.
3. H. Bohm, K. Ehrlich and K. H. Krammer, " Das Ausscheidungsverhalten der Nickellegierung Inconel 625", Metall, 24 (1970), 139–144.
4. F. Garzarotli, A. Gerscha and F. P. Francke, " Untersuchungen uber das Ausscheidungsverhalten und die mechanischen Eigenschaften der Legierung Inconel 625", Z. Metallkunde, 60(1969), 643–652.
5. M.Sundararaman, P. Mukhopadhyay and S. Banerjee," Precipitation of the δ–Ni_3Nb Phase in Two Nickel Base Superalloys", Metall. Trans., 19A (1988), 453–465.
6. R. B. Nicholson," Nucleation at Imperfections", Phase Transformations, (ASM, Metals Park, Ohio, 1970), 269–312.
7. D. Vaughan," Grain Boundary Precipitation in an Al–Cu Alloy", Acta Metall., 16 (1968), 563–577.

8. K. C. Russell and H. I. Aaronson, " Sequence of Precipitate Nucleation", J. Mater. Sci., 10 (1975), 1991–1999.
9. H. B. Aaron and H. I. Aaronson, " Altering the Time Cycle of Heat Treatment by Controlling Grain Boundary and Sub–boundary Structure", Metall. Trans.,2 (1971), 23–37.
10. E.Hornbogen and M. Roth, " Die Verteilung Koharenter Teilchen in Nickellegierungen", Z. Metallkunde, 58 (1967), 842–855.
11.J. W. Cahn, " Nucleation on Dislocations", Acta Metall., 5 (1957), 169–172.
12. R. Gomez – Ramirez and G. M. Pound, " Nucleation of Second Solid Phase on Dislocations", Metall. Trans., 4 (1973), 1563–1570.
13. F. C. Larche, " Nucleation and Precipitation on Dislocations", Dislocations in Solids, vol.4, ed.F. R. N. Nabarro,(North Holland Publishing Company, Amsterdam, 1979), 135–153.
14. M. Sundararaman and P. Mukhopadhyay, " Heterogeneous Precipitation of the γ" Phase in Inconel 625", Materials Science Forum, 3 (1985), 273–280.
15. M. Sundararaman, P. Mukhopadhyay and S. Banerjee, " Some Aspects of the Precipitation of Intermetallic Phases in Inconel 718 Alloy", Metall. Trans., 23A (1992), 2015–2028.
16. M. Sundararaman, " Microstructural Studies on the High Temperature Materials – Inconel 625 and Inconel 718 Alloys", (Ph. D. thesis, Bombay University, 1986), 152–171.
17. M. Sundararaman and P. Mukhopadhyay, " Intermetallic Phase Precipitation Behaviour of Two Wrought Nickel Base Superalloys", Metals, Materials and Processes, 3 (1991), 1–14.
18. D. E. Wenschoff, Technical Service Memorandum, (Huntington Alloys Products Division, The International Company,Huntington,WV, U.S.A., 1974).
19. E.Schabel, H. J. Schuller and P. Schwab, " The Precipitation and the Recrystallisation Behaviour of the Nickel Base Alloy Inconel 625", Practical Metallography, 8 (1971), 521–527.
20. A. K. Sinha, " Close Packed Ordered A_3B Structures in Ternary Alloys of Certain Transition Metals", Trans. TMS–AIME, 245(1969), 911–917.
21. A. Kelly and R. B. Nicholson, " Precipitation Hardening", Prog Mater. Sci., 10 (1963), 237–247.
22. G. W. Lorimer, " Precipitate Nucleation", Mater. Sci. Forum, 3 (1985), 199–209.
23. F. Kroupa, " The Interaction between Prismatic Dislocation Loops and Straight Dislocations", Philos. Mag., 7 (1962), 783–801.
24. M. J. Makin, " The Long Range Forces Between Dislocation Loops and Dislocations", Philos. Mag., 10 (1964),695–711.
25. T. Misfune and M. Meishi, "An Elasticity Calculation of the Interaction between a Misfit Defect and an Extended Dislocation in FCC Crystals", Acta Metall., 17 (1969), 1253–1262.
26. V. Gerold, " On Calculation of CRSS of Alloys Containing Coherent Precipitates", Acta Metall., 16 (1968), 823–827.
27. R. L. Fleischer, " Solution Hardening by Tetragonal Distortions: Application to Irradiation Hardening in F.C.C. Crystals", Acta Metall., 10 (1962), 835–842.
28. M. S. Bapna and V. R. Parameswaran, " Anisotropic Elastic Interaction between Misfit Defects and Extended Screw Dislocations in FCC Metals", J. Appl. Phys., 51 (1980), 3186–3193.
29. P. S. Kotval, " Carbide Precipitation on Imperfections in Superalloy Matrices", Trans. TMS–AIME, 242 (1968), 1651–1656.
30. R. L. Fleischer, " Solution Hardening", Acta Metall., 9 (1961), 996–1000.